Thin Solid Films 583 (2015) 76–80

Contents lists available at ScienceDirect

Thin Solid Films

journal homepage: www.elsevier.com/locate/tsf

Manganite based memristors: Influence of the electroforming polarity on the electrical behavior and radiation hardness

D. Rubi [a,b,c,*], A. Kalstein [a,b], W.S. Román [a,b], N. Ghenzi [a,b], C. Quinteros [a,b], E. Mangano [d], P. Granell [d], F. Golmar [b,c,d], F.G. Marlasca [a], S. Suarez [b,e], G. Bernardi [b,e], C. Albornoz [a], A.G. Leyva [a,c], P. Levy [a,b]

[a] GIyA and INN, CNEA, Av. Gral Paz 1499, (1650), San Martín, Buenos Aires, Argentina
[b] Consejo Nacional de Investigaciones Científicas y Técnicas (CONICET), Argentina
[c] Escuela de Ciencia y Tecnología, UNSAM, Campus Miguelete, (1650), San Martín, Buenos Aires, Argentina
[d] INTI, CMNB, Av. Gral Paz 5445 (B1650KNA), San Martín, Buenos Aires, Argentina
[e] Centro Atómico Bariloche (CNEA), Av. E. Bustillo km 9500 (8400), S. C. de Bariloche, Río Negro, Argentina

ARTICLE INFO

Article history:
Received 15 August 2014
Received in revised form 9 March 2015
Accepted 20 March 2015
Available online 27 March 2015

Keywords:
Oxide thin films
Resistive Random Access Memory
Radiation hardness

ABSTRACT

We report on the fabrication and characterization of $La_{2/3}Ca_{1/3}MnO_3$ manganite-based memristive devices. Polycrystalline manganite thin films were grown by Pulsed Laser Deposition, while metallic electrodes were deposited by sputtering. We show that, depending on the polarity of the initial electroforming, both clockwise and anti-clockwise current–voltage curves can be obtained. We attribute this behavior to the coexistence of different resistive switching mechanisms. We finally evaluate the electrical behavior of our devices after irradiation with high energy oxygen ions. We find no significant difference in the dielectric breakdown voltages between irradiated and non-irradiated devices, indicating that they may present radiation hardness and could be therefore appropriate for space or nuclear applications.

1. Introduction

Numerous oxides, both simple and complex, present electrical field induced Resistance Switching (RS), i.e. the reversible change of their resistance state by applying electrical stress [1–3]. This resistance change is non-volatile, and exhibits low power consumption, high retention times, high endurance and good temperature stability, turning these materials into potentially good candidates to be used in the development of Resistive Random Access Memories (ReRAM) [4].

A typical RS device, usually called "memristor", consists on an insulating or semiconductor oxide sandwiched between two metallic electrodes. RS is usually ascribed to two mechanisms: (i) formation and rupture of conducting nanofilaments bridging both electrodes and (ii) an interfacial mechanism associated with the electrical field induced movement of oxygen vacancies near the metal–oxide interface. The first mechanism is usually reported in simple oxides, while the second one is more frequently found in complex oxides. However, the previous classification is not fully consistent with all reported systems and exceptions are found in the literature [5].

Perovskite manganites with general formula $ReAMnO_3$ (Re: rare earth ions, A: alkaline ions) are strongly correlated electron systems and have been intensively studied in the last 20 years, from the discovery of the so-called colossal magnetoresistance (CMR) [6,7]. Also, from the initial report by Ignatiev et al. [8] on $Pr_{0.7}Ca_{0.3}MnO_3$ thin films, many studies dealing with the RS behavior of both ceramics and thin films of different manganites have been performed [9–12]. In addition, phenomenological models explaining the electrical behavior of these systems have been developed [13,14].

We have recently shown that an optimum RS behavior is achieved in $La_{2/3}Ca_{1/3}MnO_3$ manganite thin films with oxygen deficiency [15], evidencing the key role played by oxygen vacancies in the resistance change under electrical stimulus. Later, we have found on the same system a crossover between an interfacial RS mechanism and a filamentary regime, controlled by the compliance current (CC), externally programmed to avoid device damage during the transition from high to low resistance [16]. This finding supports the idea that, in general, most devices will present coexistence of several resistive switching mechanisms [17], being necessary a careful study in each system in order to disentangle them.

As RS based memory devices are not relying on charge storage (as FLASH based memories do) but on the change of a physical property of the oxides, these ReRAM devices should present enhanced radiation hardness, thus making them specially suited for space or nuclear applications. Indeed, we have recently shown that this is the case for TiO_2 microstructured devices [18].

In the present paper we show that different RS mechanisms can be tailored by either positive or negative electroforming (i.e. the initial electrical stress applied to virgin devices until soft electrical breaking is achieved). We also study the variation of the electrical breakdown

* Corresponding author.
E-mail address: diego.rubi@gmail.com (D. Rubi).

http://dx.doi.org/10.1016/j.tsf.2015.03.048
0040-6090/

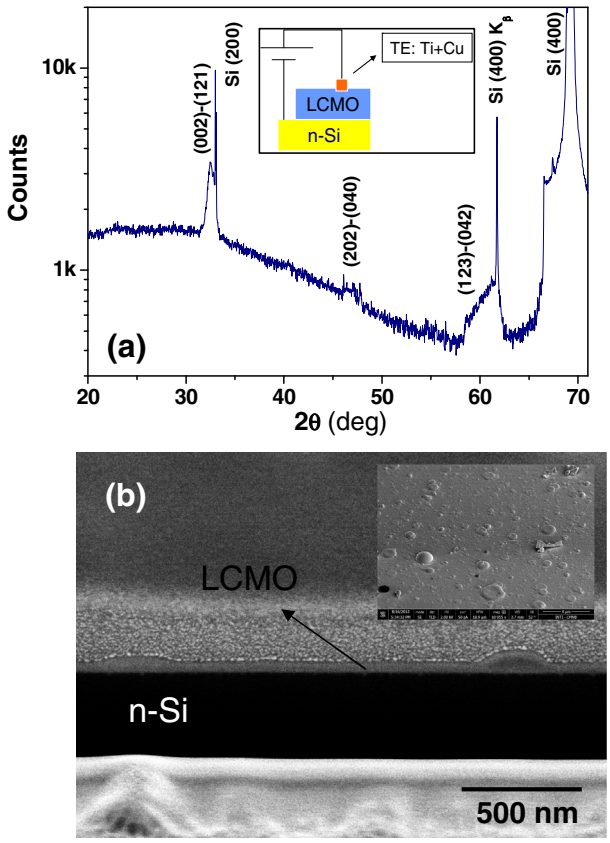

Fig. 1. (a) X-ray diffraction pattern corresponding to an LCMO thin film on n-Si. The LCMO peaks were indexed according to the bulk *Pnma* orthorhombic structure. The inset shows a sketch depicting the structure of the fabricated memristive device; (b) scanning electron microscopy cross-view image of an LCMO thin film on n-Si. The cross-section was exposed after etching with a focused ion beam. The inset displays a plane view of the same film.

voltages in devices irradiated with oxygen ions, showing that our devices present indeed radiation hardness.

2. Experimental details

$La_{2/3}Ca_{1/3}MnO_3$ (LCMO) manganite powders were prepared by using the liquid-mix method. A target was fabricated by pressing the obtained powders at 10 t, followed by a sintering in air at 1400 °C for 2 h. LCMO thin films were grown by pulsed laser deposition (pulsed Q-switched Spectra Physics Laser with $\lambda = 266$ nm and a frequency of 10 Hz) at an oxygen pressure of 13 Pa and a substrate temperature of 650 °C. The target-substrate distance was fixed at 7 cm. Films were grown on top of (conductive) n-type silicon, which also acted as bottom electrode. We used as top electrode a bilayer of sputtered Ti (10 nm) and Cu (100 nm), shaped by means of optical lithography. The top electrode areas ranged between 0.049 mm^2 and 0.785 mm^2. X-ray diffraction experiments were performed by means of an Empyrean (Panalytical) diffractometer with a Pixcel 3D detector, in standard Bragg–Brentano configuration. Both the surface and the cross-section of the films were visualized with a Scanning Electron Microscope/Focused Ion Beam (SEM/FIB) dual beam system (FEI Helios Nanolab 650), operated at a 2 kV voltage. A small volume of material was physically removed with the ion beam, and the remaining cross-section was visualized with the SEM column, with the sample tilted 52°. The electrical characterization was performed with a Keithley 2612 source-meter hooked to a probe station. The acquisition software was programmed on the LabView environment. We have irradiated selected samples with a beam of 2 MeV O^{2+} delivered by a NEC Pelletron 5SHD [19] accelerator system. O^{2-} ions were extracted from the SNICS II ion source from a cathode of Al_2O_3. Then, a charge $q = 2+$ was selected after stripping at the high voltage terminal with 2 MeV energy and beam intensities from 1 to 4 nAmps. A collected charge of 1 μC in a spot 2 mm diameter corresponds to a dose of 2×10^{14} ions/cm^2.

3. Results and discussion

LCMO thin films resulted single phase and polycrystalline, as shown in the X-ray pattern of Fig. 1(a). Fig. 1(b) shows a SEM cross-section of a LCMO thin film, showing a non-homogeneous thickness, ranging between 55 and 100 nm. Regions with higher thickness are related to the presence of nanometric particulate (better appreciated in the plane view shown in the inset of Fig. 1(b)), which is usually found on thin films grown by pulsed laser deposition [20]. EDAX experiments showed that the chemical composition of the particulate is, within the error of the technique, similar to the one of the films and consistent with the nominal stochiometry.

We turn now to the electrical properties. The inset of Fig. 1(a) displays a sketch of our devices. We have recorded simultaneously, at room temperature, pulsed current–voltage (I–V) curves and Hysteresis Switching Loops (HSL). The pulsed I–V curve consists of applying a sequence of voltage pulses of different amplitudes, with a time–width of few milliseconds and a step of 50 mV, while the current is measured during the application of the pulse. In addition, after the application of

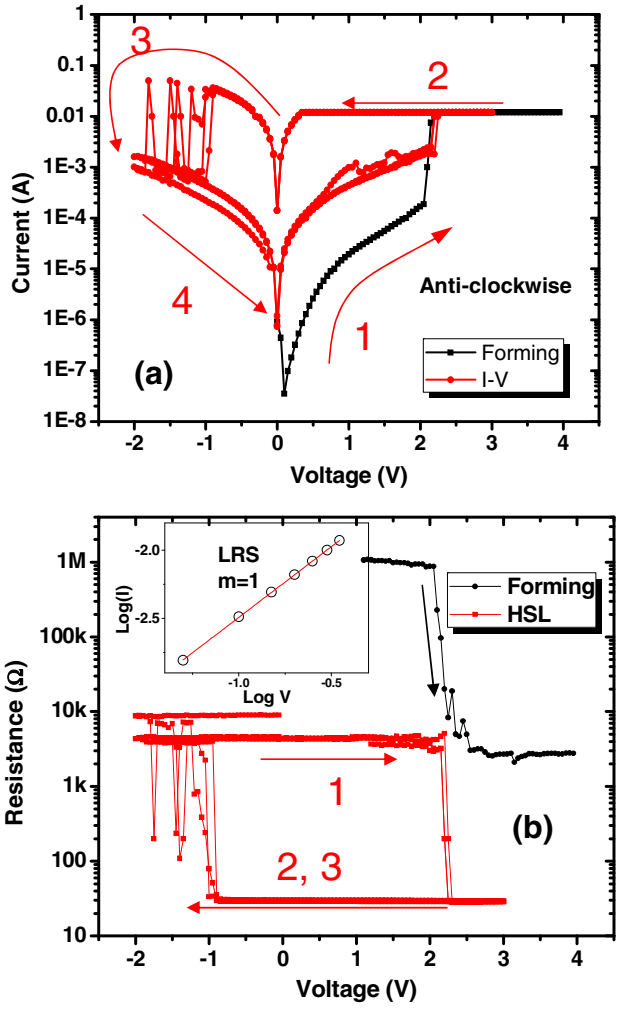

Fig. 2. (a) Initial electroforming and subsequent dynamic I–V curve obtained after stressing with positive voltage. An anti-clockwise behavior is found; (b) corresponding hysteresis switching loop, recorded by applying small voltage bias of 100 mV. The inset displays the LRS of the I–V curve in log–log scale.

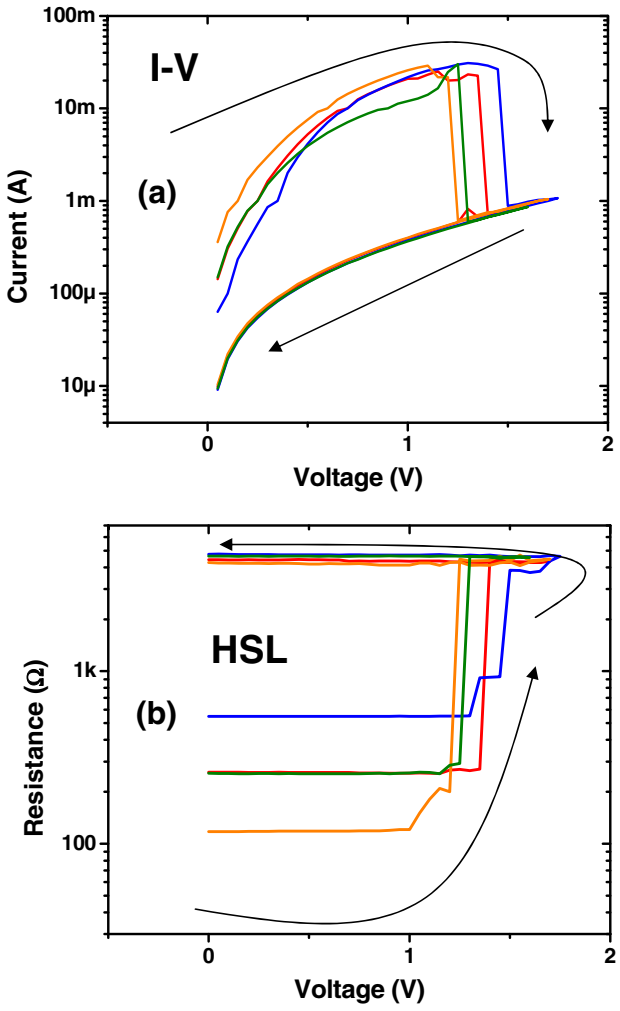

Fig. 3. (a) I–V curve showing different RESET processes obtained with positive voltage, for a positively electroformed device. The intermediate SET processes are not shown for sake of clarity; (b) corresponding remanent resistance values, measured with a voltage bias of 100 mV.

each of these pulses we apply a small undisturbing reading voltage of 100 mV that allows us to evaluate the remnant resistance state (HSL). Figs. 2(a) and 2(b) display the dynamic I–V curve and HSL, corresponding to a device initially stressed with positive voltage. It is found that the sample presents a virgin resistance of around 2 MΩ; when a voltage of +2.3 V is reached, the electroforming process takes place and the resistance suddenly drops to 10 kΩ. Further stable RS between high (5–10 kΩ, HRS) and low (30 Ω, LRS) resistance states can be observed. The SET (transition from HRS to LRS) voltages are found between +2 and +2.5 V, while the RESET voltages (transition from LRS to HRS) are observed between −1 and −2 V. As previously reported [16], the RS mechanism in the case of positive electroforming can be related to the movement of oxygen vacancies near the top electrode–manganite interface, or it may be associated to the diffusion of the top electrode through the oxide until a metallic nanofilament bridging both electrodes is formed. In the present case, different evidences point to the latter mechanism dominating the RS behavior: (i) the lack of dependence of the LRS with the area of the top electrode (not shown here), suggesting a highly inhomogeneous conducting path; (ii) a concomitant and monotonous decrease of both LRS and HRS with increasing SET CC (values between 10 mA to 200 mA were swept, not shown here), suggesting the formation of stronger filaments which are more difficult to break upon increasing the CC; and (iii) the possibility of getting RESET transitions with positive voltage, as shown in Fig. 3. This figure displays several runs where positive RESETs are obtained after positive SETs (the SETs are not shown for sake of clarity). The described behavior suggests a RESET mechanism associated to filament rupture by Joule heating (independent of the current direction), in a fuse-like mechanism. On the other hand, we recall that the slope of the LRS branch in the log–log I–V curve is a signature of the involved mechanism ($m \sim 1$ suggests filamentary conduction, while $m \sim 2$ is an evidence of interfacial behavior [16]). In the case of samples reported here, as shown in the inset of Fig. 2(b), we obtained $m \sim 1$ when varying the CC in the range 10 mA to 200 mA. This result is different to the one reported in Ref. [16], where a crossover regime (from $m = 2$ to $m = 1$) was attained for CC around 90 mA. Samples reported here are thinner and exhibit a higher density of particulate than samples reported in Ref. [16]. The latter suggests an increased presence of grain boundaries, making the top electrode diffusion easier under relatively lower electrical fields. In this way, the filamentary regime is stabilized faster and dominates in the whole range of explored CCs.

Fig. 4 shows both the dynamic I–V curve and HSL obtained after initially stressing a virgin device with a negative voltage. The inset of Fig. 4(a) shows that a negative electroforming is achieved at a voltage of around −2 V, the resistance changing from ~5 MΩ to ~50 kΩ. When further pulsed voltage ramps are applied, it is found that the system reversibly changes between high (~1 MΩ) and low (~10 kΩ) resistance states, as shown in Fig. 4(a) and (b). The SET voltages are

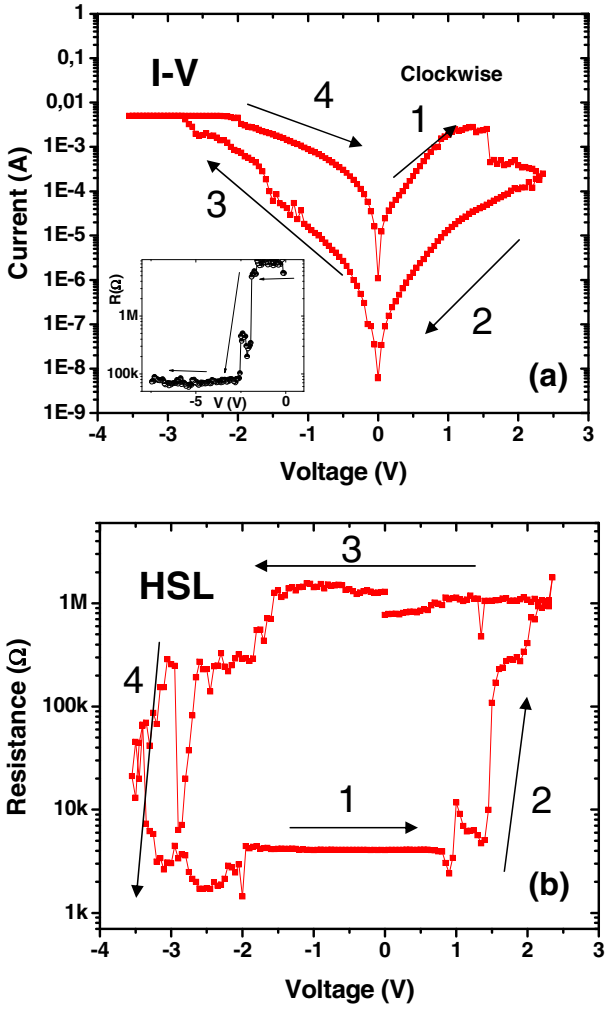

Fig. 4. (a) The inset shows the initial electroforming after stressing the virgin sample with negative voltage. The main panel display subsequent dynamic I–V curves. A clockwise behavior is found; (b) corresponding hysteresis switching loop, recorded by applying small voltage bias of 100 mV.

between −2 and −3 V, while the RESET voltages are around +1.5 V. It should be noted that the I–V curve displays in this case a clockwise behavior in the positive voltage quadrant, on the contrary to the previous case (positive electroforming), which displayed and anti-clockwise behavior. This strongly suggests that different RS mechanisms are operative in each case [21]. Going back to the negative electroforming case, we should point that a negative polarity applied to the top electrode inhibits the migration of top electrode metal, suggesting the absence of a filamentary process. Also, a negative voltage applied to the top electrode would attract positively charged oxygen vacancies, increasing the resistance of the top electrode–manganite interface. This is in contrast to the observed decrease of resistance upon negative voltage stressing. Therefore, it is reasonable to assume that the dominant switching mechanism in the case of the negative electroforming is related to modifications in the Si–manganite interface. A possible scenario is related to the electric field induced oxidation and reduction of the native (~1 nm thick) SiO_x layer present at the Si–manganite interface [21]. Indeed, it has been shown that such an ultrathin layer can origin RS [22]. The proportionality between the low resistance state obtained after negative electroforming and the inverse of the top electrode area (not shown here) supports the existence of a RS mechanism distributed all along the device area, consistently with the mechanism proposed above.

In order to test the effect of irradiation on the electrical properties of the films, we have compared the soft dielectric breakdown voltages, of both irradiated and non-irradiated devices. For these experiments we have grown a new series of LCMO samples on n-Si with Ti top electrodes (120 nm thick). One column of devices with different areas was irradiated with 2 MeV oxygen ions until a dose of 2×10^{14} ions/cm^2 was achieved. The remaining devices were shielded and used as blank, i.e., they were exposed to the same atmospheric conditions and electrical testing protocol, but not to the ions. The experiment started with virgin devices, which were progressively stressed under either positive or negative voltages until breakdown was observed (see Fig. 5(a)). The collected breakdown voltages are depicted in Fig. 5(b). It can be seen that the negative and positive breakdown voltages, when plotted as a function of the device area for both irradiated and non-irradiated samples, do not follow any clear trend, displaying roughly constant (averaged) values at −3.4(2) V and 2.0(4) V. This provides a first clue about our LCMO-based devices presenting radiation hardness, for the dose applied in the present work, which turns them attractive for possible space or nuclear applications. Further studies in order to confirm this issue are being performed and will be reported in the future.

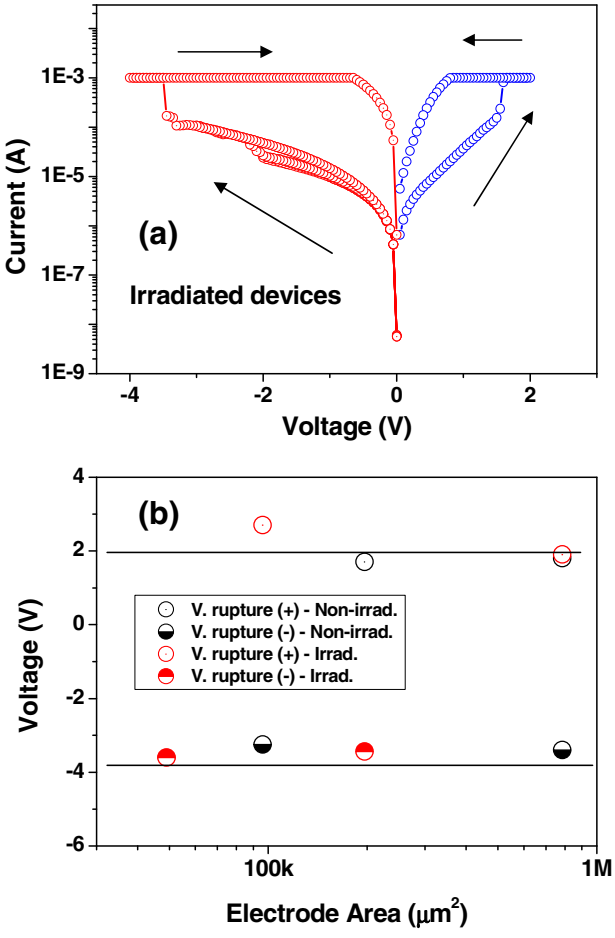

Fig. 5. (a) I–V curve for positive and negative stimuli for two irradiated devices. The voltage was raised until dielectric breakdown was observed; (b) evolution of the dielectric breakdown voltages (both positive and negative) as a function of the device area, both for irradiated and non-irradiated devices. No significant modification of these voltages is found after irradiation with high energy oxygen ions.

4. Conclusions

In summary, we have prepared and characterized LCMO manganite-based memristive devices. We have shown the coexistence of different resistive switching mechanisms. Each mechanism can be activated by controlling the electroforming polarity. We finally have shown that the dielectric breakdown voltages for both positive and negative polarities are not affected by irradiation with high energy oxygen ions, suggesting that our devices present radiation hardness properties.

Acknowledgments

We acknowledge financial support from CONICET (PIPs 291, 216 and "MeMO"), PICT 0788 "MeMO" and CIC—Buenos Aires. We thank Dr. D. Vega, from the Laboratory of X-ray Diffraction (GIA, GAIyANN, CAC, CNEA) for the XRD measurements.

References

[1] R. Waser, R. Dittmann, G. Staikov, K. Szot, Redox-based resistive switching memories—nanoionic mechanisms, prospects, and challenges, Adv. Mater. 21 (2009) 2632.
[2] A. Sawa, Resistive switching in transition metal oxides, Mater. Today 11 (2008) 28.
[3] M.J. Rozenberg, Resistive Switching, 2011. 11414 http://dx.doi.org/10.4249/scholarpedia.
[4] D.B. Strukov, H. Kohlstedt, Resistive switching phenomena in thin films: materials, devices, and applications, MRS Bull. 37 (2012) 108.
[5] J.J. Yang, I.H. Inoue, T. Mikolajick, C.S. Hwang, Metal oxide memories based on thermochemical and valence change mechanisms, MRS Bull. 37 (2012) 131.
[6] S. Jin, T.H. Tiefel, M. McCormack, R.A. Fastnacht, R. Ramesh, L.H. Chen, Thousandfold change in resistivity in magnetoresistive La–Ca–Mn–O films, Science 264 (1994) 413.
[7] A. Asamitsu, Y. Tomioka, H. Kuwahara, Y. Tokura, Current switching of resistive states in magnetoresistive manganites, Nature 388 (1997) 50.
[8] S.Q. Liu, N.J. Wu, A. Ignatiev, Electric-pulse-induced reversible resistance change effect in magnetoresistive films, Appl. Phys. Lett. 76 (2000) 2749.
[9] M. Quintero, A.G. Leyva, P. Levy, Simultaneous electric and magnetic field induced nonvolatile memory, Appl. Phys. Lett. 86 (2005) 242102.
[10] N. Das, S. Tsui, Y.Y. Xue, Y.Q. Wang, C.W. Chu, Electric-field-induced submicrosecond resistive switching, Phys. Rev.B 78 (2008) 235418.
[11] Ch. Jooss, J. Hoffmann, J. Fladerer, M. Ehrhardt, T. Beetz, L. Wu, Y. Zhu, Electric pulse induced resistance change effect in manganites due to polaron localization at the metal–oxide interfacial region, Phys. Rev. B 77 (2008) 132409.
[12] N.A. Tulina, S.A. Zverkov, Y.M. Mukovskii, D.A. Shulyatev, Current switching of resistive states in normal-metal-manganite single-crystal point contacts, Europhys. Lett. 56 (2001) 836.
[13] M. Quintero, P. Levy, A.G. Leyva, M.J. Rozenberg, Mechanism of electric-pulse-induced resistance switching in manganites, Phys. Rev. Lett. 98 (2007) 116601.
[14] M.J. Rozenberg, M.J. Sánchez, R. Weht, C. Acha, F. Gomez-Marlasca, P. Levy, Mechanism for bipolar resistive switching in transition-metal oxides, Phys. Rev. B 81 (2010) 115101.
[15] I. Alposta, A. Kalstein, N. Ghenzi, S. Bengio, G. Zampieri, D. Rubi, P. Levy, Resistive switching in ferromagnetic $La_{2/3}Ca_{1/3}MnO_3$ thin films, IEEE Trans. Magn. 49 (2013) 4582.

[16] D. Rubi, F. Tesler, I. Alposta, A. Kalstein, N. Ghenzi, F. Gomez-Marlasca, M. Rozenberg, P. Levy, Two resistive switching regimes in thin film manganite memory devices on silicon, Appl. Phys. Lett. 103 (2013) 163506.
[17] N. Ghenzi, M.J. Sánchez, D. Rubi, M.J. Rozenberg, C. Urdaniz, M. Weissman, P. Levy, Tailoring conductive filaments by electroforming polarity in memristive based TiO_2 junctions, Appl. Phys. Lett. 14 (2014) 183505.
[18] N. Ghenzi, D. Rubi, E. Mangano, G. Gimenez, J. Lell, A. Zelcer, P. Stoliar, P. Levy, Building memristive and radiation hardness TiO_2-based junctions, Thin Solid Films 550 (2014) 683.
[19] S. Limandri, C. Olivares, L. Rodriguez, G. Bernardi, S. Suárez, PIXE facility at Centro Atómico Bariloche, Nucl. Inst. Methods Phys. Res. B 318 (2014) 47.
[20] Douglas B. Chrisey, Graham K. Hubler, Pulsed Laser Deposition on Thin Films, John Wiley & Sons, New York, 1994.
[21] G. Jian-Lei, L. Song-Lin, L. Zhao-Liang, M. Yang, L. Xue-Jin, C. Dong-Min, Clockwise vs counter-clockwise I–V hysteresis of point-contact metal-tip/$Pr_{0.7}Ca_{0.3}MnO_3$/Pt devices, Chin. Phys. Lett. 27 (2010) 027301.
[22] C. Li, H. Jiang, Q. Xia, Low voltage resistive switching devices based on chemically produced silicon oxide, Appl. Phys. Lett. 103 (2013) 062104.